Oermann, Michael Raymond; Ebendorff-Heidepriem, Heike; Li, Yahua; Foo, Tze Cheung; Monro, Tanya Mary.
Index matching between passive and active tellurite glasses for use in microstructured fiber lasers: Erbium doped lanthanum-tellurite glass, *Optics Express*, 2009; 17(18):15578-15584.

# Index matching between passive and active tellurite glasses for use in microstructured fiber lasers: Erbium doped lanthanum-tellurite glass

**Michael R. Oermann,* Heike Ebendorff-Heidepriem, Yahua Li, Tze-Cheung Foo, Tanya M. Monro**

*Centre of Expertise in Photonics, School of Chemistry & Physics, University of Adelaide, Adelaide, SA 5005, Australia*

**michael.oermann@adelaide.edu.au*

**Abstract:** Active and passive variants of La-containing tellurite glasses have been developed with matched refractive indices. The consequences of adding lanthanum to the glass was studied through measurements of the crystallization stability, glass viscosity and the loss of unstructured fibers. Doping the glass with erbium allowed for any spectroscopic changes to be observed through measurements of the absorption and energy level lifetimes. The fluorescence emission spectra were measured at 1.5 μm and, to the best of our knowledge, for the first time in tellurite glass at 2.7 μm.



**OCIS codes:** (160.2290) Fiber Materials; (160.5690) Rare-earth-doped materials; (160.3380) Laser materials

## References and links

1. A. Mori, Y. Ohishi, and S. Sudo, "Erbium-doped tellurite glass fibre laser and amplifier," Electron. Lett. **33**(10), 863–864 (1997).
2. B. Richards, Y. Tsang, D. Binks, J. Lousteau, and A. Jha, "Efficient ~2μm $Tm^{3+}$-doped tellurite fiber laser," Opt. Lett. **33**(4), 402–404 (2008).
3. Y. Tsang, B. Richards, D. Binks, J. Lousteau, and A. Jha, "$Tm^{3+}$/$Ho^{3+}$ codoped tellurite fiber laser," Opt. Lett. **33**(11), 1282–1284 (2008).
4. J. S. Wang, E. M. Vogel, and E. Snitzer, "Tellurite glass: new candidate for fiber devices," Opt. Mater. **3**(3), 187–203 (1994).
5. T. M. Monro, and H. Ebendorff-Heidepriem, "Progress in microstructured optical fibers," Annu. Rev. Mater. Res. **36**(1), 467–495 (2006).
6. K. Patek, *Glass Lasers*, (CRC Press, 1970)
7. A. H. Raouf, El-Mallawany, *Tellurite Glasses Handbook: physical properties and data*, (CRC Press, 2002)
8. G. Nunzi Conti, V. K. Tikhomirov, M. Bettinelli, S. Berneschi, M. Brenci, B. Chen, S. Pelli, and A. Speghini, "Characterization of ion-exchanged waveguides in tungsten tellurite and zinc tellurite $Er^{3+}$-doped glasses," Opt. Eng. **42**(10), 2805–2811 (2003).
9. L. Li, A. Schülzgen, V. L. Temyanko, H. Li, S. Sabet, M. M. Morrell, A. Mafi, J. V. Moloney, and N. Peyghambarian, "Investigation of modal properties of microstructured optical fibers with large depressed-index cores," Opt. Lett. **30**(24), 3275–3277 (2005).
10. S. Dai, C. Yu, G. Zhou, J. Zhang, G. Wang, and L. Hu, "Concentration quenching in erbium-doped tellurite glasses," J. Lumin. **117**(1), 39–45 (2006).
11. T. A. Birks, J. C. Knight, and P. S. Russell, "Endlessly single-mode photonic crystal fiber," Opt. Lett. **22**(13), 961–963 (1997).
12. H. Ebendorff-Heidepriem, and T. M. Monro, "Extrusion of complex preforms for microstructured optical fibers," Opt. Express **15**(23), 15086–15092 (2007).
13. E. Roeder, "Extrusion of glass," J. Non-Cryst. Solids **5**(5), 377–388 (1971).
14. M. Braglia, S. Mosso, G. Dai, E. Billi, L. Bonelli, M. Baricco, and L. Battezzati, "Rheology of tellurite glasses," Mater. Res. Bull. **35**(14-15), 2343–2351 (2000).
15. G. Ghosh, "Sellmeier coefficients and chromatic dispersions for some tellurite glasses," J. Am. Ceram. Soc. **78**(10), 2828–2830 (1995).
16. S. Shen, A. Jha, E. Zhang, and S. J. Wilson, "Compositional effects and spectroscopy of rare earths ($Er^{3+}$, $Tm^{3+}$, and $Nd^{3+}$) in tellurite glasses," C. R. Chim. **5**(12), 921–938 (2002).
17. H. Ebendorff-Heidepriem, D. Ehrt, M. Bettinelli, and A. Speghini, "Effect of glass composition on Judd-Ofelt parameters and radiative decay rates of $Er^{3+}$ in fluoride phosphate and phosphate glasses," J. Non-Cryst. Solids **240**(1-3), 66–78 (1998).

18. R. S. Grew, H. Ebendorff-Heidepriem, P. J. Veitch, and T. M. Monro, "Concentration effects in erbium doped tellurite glass," Proc. COMMAD, 196–199 (2006).
19. R. Reisfeld, and Y. Eckstein, "Radiative and non-radiative transition probabilities and Quantum yields for excited states of $Er^{3+}$ in germanate and tellurite glasses," J. Non-Cryst. Solids **15**(1), 125–140 (1974).
20. H. Kühn, S. T. Fredrich-Thornton, C. Kränkel, R. Peters, and K. Petermann, "Model for the calculation of radiation trapping and description of the pinhole method," Opt. Lett. **32**(13), 1908–1910 (2007).
21. H. Ebendorff-Heidepriem, T. C. Foo, Y. Li, M. R. Oermann, T. M. Monro, "New tellurite glasses for erbium fibre lasers," proc. OECC/ACOFT, paper TuD-2 (2008)
22. R. Rolli, M. Montagna, S. Chaussedent, A. Monteil, K. Tikhomirov, and M. Ferrari, "Erbium-doped tellurite glasses with high quantum efficiency and broadband stimulated emission cross section at 1.5μm," Opt. Mater. **21**(4), 743–748 (2003).
23. H. Ebendorff-Heidepriem, D. Ehrt, J. Philipps, T. Topfer, A. Speghini, M. Bettinelli, and R. W. S. Fat, "Properties of $Er^{3+}$ Doped Glasses for Waveguide and Fiber Lasers," Proc. SPIE **3942**, 29–39 (2000).

## 1. Introduction

Tellurite glasses are promising hosts for fiber lasers operating in the mid-IR [1–3]. They have low phonon energies, high refractive indices, high rare earth solubility, infrared transmission up to 5 μm and high gain per unit length [4]. Compared to fluoride glasses, which also feature low phonon energies, they exhibit a higher thermal stability and improved corrosion resistance [4]. In this paper, erbium was used as the rare-earth dopant as it can be pumped with commercially available diode lasers at 790 nm and 980 nm and emits in the mid-IR.

Microstructured optical fiber (MOF) technology [5] is a promising route to high power double-clad tellurite fiber lasers. Holey claddings offer novel properties such as the combination of large mode area, high power transmission without damage and single mode guidance at all wavelengths [5]. Cladding pumping requires the active dopant(s) to be confined to the core region. The refractive index of the active region must therefore closely match to that of the passive glass. It is well known that doping silicate glasses with rare earth ions increases the refractive index (n) [6]. In contrast to silicate glasses ($n\approx1.5$), tellurite glasses have higher refractive indices ($n\approx2.0$) and considerably higher polarizability [7]. When doping tellurite glass, the tellurium ions are replaced by rare earth ions which have a lower polarizability. As a result the Er-doped tellurite glass has a lower refractive index than the undoped glass [8]. This is of particular importance when doping only the core of a MOF as the refractive index of the core may be reduced to below the effective index of the holey cladding, thus preventing index guiding. The guidance can be restored by increasing the air fraction of the microstructure in the cladding [9], or by modifying the composition of the core and cladding glasses to minimize the difference in their refractive indices. The addition of $La_2O_3$ to a tellurite glass promises index matching between undoped and rare earth doped glasses. The $La^{3+}$ ions have similar properties to the active rare earth ions, such as $Er^{3+}$, but do not absorb in the same wavelength range. The potential of $La_2O_3$ for index matching in tellurite glass is illustrated by the bulk glass measurements reported in Ref [10].

The $5Na_2O$-$20ZnO$-$75TeO_2$ tellurite glass composition was demonstrated to be a promising host for rare-earth doped lasers [4]. In this paper, we explore the potential of this glass composition (hereafter referred to as base glass) for the development of a core doped tellurite MOF, using erbium as the active ion. We demonstrate that modification of the cladding structure alone is insufficient to compensate for the $Er_2O_3$ induced refractive index decrease, whereas addition of $La_2O_3$ to the base glass enables index matching between the Er-doped core and passive cladding glass. The thermal and optical properties of the undoped and Er-doped La-Na-Zn-tellurite glass (hereafter referred to as La-glass) are compared with the undoped and Er-doped base glass. The suitability of the La-glass for low-loss fiber fabrication is demonstrated via bare fibers made using the extrusion technique for preform fabrication.

## 2. Modeling of tellurite MOFs

The effective refractive index of the cladding region can be approximated by the effective index of the fundamental space filling mode (FSM) that would propagate through an infinite variant of the cladding lattice [11]. The impact of increasing the air fraction of the cladding microstructure on its effective index was modeled by increasing $d/\Lambda$ (d = hole diameter and $\Lambda$

= hole to hole spacing) of a variety of hexagonally periodic cladding geometries. The modeled structures had $\Lambda = 20\mu m$ and varied hole diameters resulting in d/Λ's ranging from 0.3 up to 0.7. For fibers made solely from the host glass, increasing d/Λ across this range would cause the difference in refractive index (Δn) between the core and the numerically calculated FSM index for the cladding region to increase from $1.5\times10^{-4}$ for d/Λ = 0.3 up to $9.8\times10^{-4}$ for d/Λ = 0.7. Evidence given in previous tellurite glass papers as well as measured refractive indices (Table 1) indicate that the refractive index change due to rare earth doping ($\Delta n = 1\times10^{-3}$ for a concentration of $1\times10^{20}$ions/cm$^3$ and $\Delta n = 7\times10^{-3}$ for a concentration of $5\times10^{20}$ions/cm$^3$) exceeds this microstructure induced Δn between the core and cladding ($1\times10^{-3}$). Hence, for a tellurite glass MOF with an Er-doped core of moderate concentration ($1.0 \times 10^{20}$ions/cm$^3$) and undoped holey cladding, guidance cannot be achieved even with a predominantly air cladding without modification to either the core or cladding glass compositions.

### 3. Glass and fiber fabrication

Modeling demonstrated that index matching via modification of the glass composition is essential to create a core doped tellurite MOF. We selected $La_2O_3$ addition as a promising approach for index matching. To explore the impact of $La_2O_3$ addition on the thermal and optical properties of glass, we prepared Er-doped and undoped base glass and Er-doped and undoped La-glass (Table 1). These glasses were melted at 900 °C in gold crucibles, cast into brass moulds and then slowly cooled to room temperature. In the Er-doped base glasses and in the undoped La-glass, $Er_2O_3$ and $La_2O_3$ were added to the base glass prior to melting. In the Er-doped La-tellurite glass some of the $La_2O_3$ was replaced by $Er_2O_3$ keeping the lanthanide ion concentration constant (Table 1). Glass blocks made from 30 g batches were used for preparation of polished glass plates of 2 mm thickness. These plates were used for refractive index, absorption and fluorescence lifetime measurements. Cylindrical glass billets of 30 mm diameter were produced from 100 g batches. These billets were used to fabricate 10 mm diameter rods using the billet extrusion technique [12] and reduced in scale on a fiber drawing tower into bare (unstructured) fibers. These bare fibers enabled the measurement of the glass loss and illustrated the suitability of this glass as a fiber material.

**Table 1. Density, refractive indices, experimentally measured and theoretically calculated $Er^{3+}$ lifetimes for undoped and Er-doped base glasses, and for undoped and Er-doped La-tellurite glasses**

| | Glass | $Ln^{3+}$ ($10^{20}$ cm$^{-3}$) | | density | Refractive index | | | Lifetime (ms) for $^4I_{13/2}$ | | Lifetime (ms) for $^4I_{11/2}$ | |
|---|---|---|---|---|---|---|---|---|---|---|---|
| | | $Er^{3+}$ | $La^{3+}$ | | 633nm | 1310nm | 1550nm | calc | meas | calc | meas |
| base glass | undoped | - | - | 5.34 | 2.0515 | - | - | - | - | - | - |
| | B-Er1 | 1 | - | 5.37 | 2.0505 | - | - | 3.4 | 3.0 | 0.23 | 0.20 |
| | B-Er5 | 5 | - | 5.40 | 2.0435 | - | - | 3.4 | 3.1 | 0.23 | 0.18 |
| La-glass | undoped | - | 10 | 5.37 | 2.0360 | 1.987 | 1.983 | - | - | - | - |
| | La-Er1 | 1 | 9 | 5.37 | 2.0355 | 1.987 | 1.983 | 3.4 | 3.1 | 0.23 | 0.21 |
| | *Error* | | | *±0.1* | | *±5×10$^{-4}$* | | *±0.3* | *±0.3* | *±0.02* | *±0.02* |

## 4. Thermal and optical properties of the glasses

### *4.1 Glass transition and crystallization stability*

To determine the thermal and crystallization stability of the base and La-glass, we measured the glass transition temperature (Tg) and crystallization onset temperature (Tx) of the glasses. The thermal stability is indicated solely by the Tg and the crystallization stability of a glass is indicated by the temperature difference ΔT=Tx-Tg. These values were measured via differential scanning calorimetry using a heating rate of 10 °C/min. The base glass had a Tg of 302 °C and ΔT of 133 °C. The La-tellurite glass had both a higher Tg (315 °C) and higher ΔT (165 °C) compared with the base glass, which is of benefit for fiber fabrication.

### *4.2 Glass viscosity*

Billet extrusion has been demonstrated to be a viable technique for the fabrication of microstructured fiber preforms [12]. This approach forces a glass billet at elevated temperature through a die into free space. To avoid glass crystallization, preform deformation and die breakage, the extrusion temperature needs to be selected with care, which requires knowledge of the temperature dependence of the glass viscosity. Simple and complex preforms are extruded in the viscosity range of $10^7$-$10^{10}$ dPa.s. In this relatively narrow range, measured temperature-viscosity-data can be well fitted with an Arrhenius equation. We used extrusion of rods from glass billets to determine the temperature-viscosity-curve for our glasses. The flow through dies with a circular channel obeys the Poiseuille law [13], which allows calculation of the glass viscosity at a fixed extrusion temperature from the extrusion speed and pressure as well as the die channel length and diameter. The temperature-viscosity-curve η(T) of the base glass has been reported previously by Braglia et al [14]. The base glass viscosity data measured here agree well with the Arrhenius equation based viscosity curve presented in Braglia's paper, proving how a rod extrusion is a suitable method for calculating a glass's viscosity. For the La-glass, the η(T) curve was calculated by fitting our measured viscosity data to an Arrhenius equation. Figure 1(a) shows that the La-tellurite glass has a higher viscosity than the base glass, which is consistent with the higher Tg of this glass. The similar viscosities of the Er-doped glasses compared with the corresponding undoped glasses indicate that, unsurprisingly, small rare earth amounts do not change the glass viscosity.

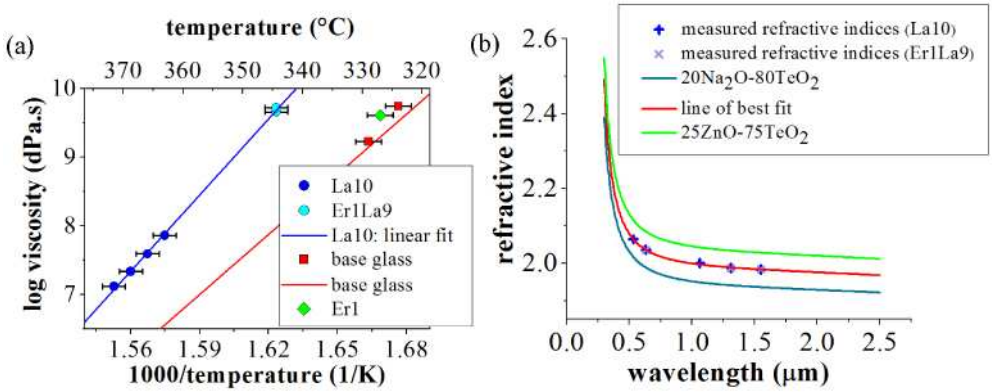


Fig. 1. (a) Glass viscosity as a function of temperature. (b) Refractive index dispersion for La-glasses, along with Sellmeier curves for two other tellurite glasses [15].

### *4.3 Refractive index*

The refractive indices of the glasses were measured using a prism coupler. The glass plates were positioned against the prism such that there was good contact. A rutile ($Ti0_2$) prism was used for these refractive index measurements as the index of the tellurite was known to lie between 2 and 2.6. The index was measured for all the samples at 632.8 nm to investigate the

$Er^{3+}$ concentration dependence on the refractive index and the La-samples were measured at a range of wavelengths (632.8nm, 1310nm and 1550nm for the Er1La9 glass and for the La10 glass also at 532nm and 1064nm) to evaluate the index matching in undoped and doped La-samples at different wavelengths. The index measurements (Table 1) verify that Er-doping of the La-free base glass reduces the refractive index, whereas the refractive index of the Er-doped La-glass closely matches that of the undoped La-glass within the measurement error. The indices of the undoped and Er-doped La-glasses are plotted against the Sellmeier curves for binary sodium tellurite and zinc tellurite glasses [15] in Fig. 1(b). It is evident that the measured refractive indices follow a similar dispersion curve.

*4.4 Bare (unstructured) fibers*

Bare (unstructured) fibers were made from undoped base glass as well as undoped and Er-doped La-glass. The bare fiber loss is a useful indicator of the glass loss, and also demonstrates the impact of La- and Er-doping on the loss. The bare fiber loss spectra (Fig. 2(a)) were measured using the standard cutback measurement technique on 200μm outer diameter bare fibers. This fiber diameter was chosen for its handleability (the ability to handle the fiber without breakage) and reproducibility in cleave quality. The fiber loss is independent of the fiber diameter as it is dominated by the material losses. A broadband white light source was collimated and then focused into the test fibers. The output signal was launched into an OSA directly using a bare fiber adaptor. Both the undoped base and La-glass bare fibers have low minimum losses of ≈0.2 ± 0.1 dB/m at 1.3 μm. The Er-doped La-glass fiber has a higher minimum loss of ≈0.4 ± 0.1 dB/m at 1.2 μm. These losses are comparable to the fiber loss measured by Shen et al [16] also for a Na-Zn-tellurite glass and demonstrate the suitability of the La-tellurite glass as a fiber material.

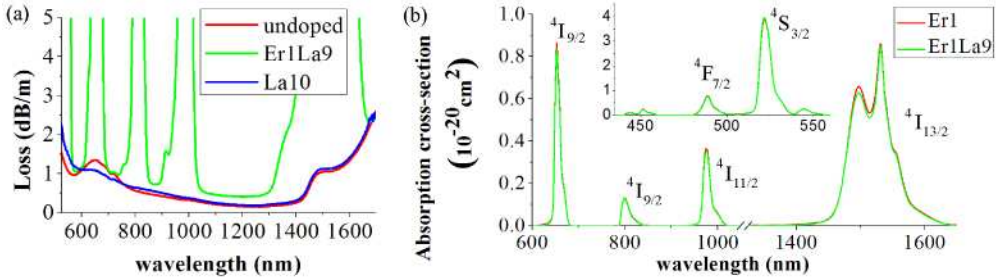


Fig. 2. (a) Loss spectra of the bare (unstructured) fiber made from undoped, La10 and Er1La9 glasses, (b) $Er^{3+}$ absorption cross-section for Er-doped base and La-tellurite glass.

## 5. Spectroscopic properties of $Er^{3+}$ in the tellurite glasses

*5.1 Absorption*

The absorption spectra in the visible to near-infrared region were measured using a CARY spectrophotometer. The absorption cross section, $\alpha$, (Fig. 2(b)) was calculated from the measured absorbance spectrum using the sample thickness and $Er^{3+}$ ion concentration. Note the area under the absorption cross-section for each energy level, $\int \alpha \, d\lambda$, is proportional to $(n^2+2)^2/9n$, where $n$ is the refractive index of the glass. A full derivation of this relationship is presented by Ebendorff-Heidepriem et al [17]. When comparing the doped base glass (B-Er1) and the doped lanthanum glass (La-Er1), which exhibit slightly different refractive indices, one would expect variation in their absorption cross-sections. According to the measured refractive indices, the lower index of the La-Er1 glass would theoretically result in a 1% reduction in the integral of its absorption cross-section, which is samller that the 5% error in the glass sample thickness measurement. Thus, the expected 1% difference between the B-Er1 and La-Er1 absorption cross-sections is not evident, and the absorption cross-

section is unchanged with the addition of lanthanum to the glass composition within the measurement error.

*5.2 Fluorescence*

The total radiative decay rate (A) and lifetime of the $Er^{3+}$ $^4I_{13/2}$ and $^4I_{11/2}$ energy levels were calculated from the absorption cross-section spectra using the Judd-Ofelt analysis [17,18]. The non-radiative multiphonon decay rate was calculated through the extrapolation of the results presented by Reisfeld et al [19] for their sodium-tellurite glass. The fluorescence lifetimes of the $Er^{3+}$ $^4I_{11/2}$ and $^4I_{13/2}$ energy levels were measured by directly pumping the $I_{11/2}$ level with a pulsed 974 nm laser and analyzing the fluorescence decay curve. The pinhole technique described by Kuhn et al [20] and a 300μm pinhole was used to minimize reabsorption effects (radiation trapping). Filters were used to observe the fluorescence decay to the ground state ($^4I_{15/2}$) for each energy level individually.

Due to the wide gap between the $^4I_{13/2}$ level and the next lower level $^4I_{15/2}$, the multiphonon decay rate for this transition ($W < 1\ s^{-1}$) is negligible compared with the radiative decay rate ($A = 290\ s^{-1}$), and thus the theoretically predicted lifetime is effectively the radiative lifetime of ≈3.4 ms. This is seen in our measurements of this level's lifetime which agree with the radiative decay time within the measurement error. For all three Er-doped glass samples, the measured lifetime of the $^4I_{13/2}$ level (Table 1) is similar to the predicted lifetime. This demonstrates that for both the base and the La-tellurite glass, concentration quenching is not significant for $Er^{3+}$ concentrations up to $5\times10^{20}$ ions/cm$^3$. This is in contrast to other tellurite glasses, where quenching of the $^4I_{13/2}$ level via energy transfer to OH groups in the glass (OH quenching) occurs from very low $Er^{3+}$ concentrations ($0.2\times10^{20}$ ions/cm$^3$) [10,16] although our tellurite glasses exhibit similar OH contents (i.e. similar OH absorption coefficients at ~3.3 μm [21]) compared to other tellurite glasses that were also melted in ambient atmosphere [10,16]. Tellurite glasses melted in a glove box under a nitrogen atmosphere also do not suffer from OH quenching for concentrations up to $5\times10^{20}$ ions/cm$^3$ [8,22]. In phosphate glasses, the OH quenching at low $Er^{3+}$ concentrations is attributed to clustering between $Er^{3+}$ ions and OH groups [23]. The absence of OH quenching in our glass indicates that the $Er^{3+}$ ions are evenly distributed and do not form clusters with OH groups.

For the $^4I_{11/2}$ to $^4I_{13/2}$ transition, the multiphonon decay rate ($W \approx 4000\ s^{-1}$) is considerably larger than the calculated radiative decay rate ($A = 370\ s^{-1}$) and thus the multiphonon decay rate is included in the theoretically predicted lifetime of 0.23 ms. For all three Er-doped glass samples, the measured lifetime of the $^4I_{11/2}$ level (Table 1) is similar to the theoretically predicted lifetime, which confirms that the lifetime of this level is shortened considerably by non-radiative decay. For the two $Er^{3+}$ energy levels considered, the base glass and La-tellurite glass samples have the same measured lifetimes within the measurement errors, which demonstrates that the addition of $La_2O_3$ does not have a detrimental impact on the $Er^{3+}$ fluorescence lifetimes.

The fluorescence was measured from a 2mm thick La-Er1 sample excited with a 974nm pump source. The spectrum (Fig. 3) was acquired using a JY Horiba spectrometer and a PbSe detector and is normalized to the peak of the characteristic 1.5μm emission. The measurement of the 2.7μm fluorescence illustrates that the decay over the 2.7μm transition is not completely quenched by non-radiative decay, although due to the shortened lifetime of this energy level, achieving population inversion across this transition will not be trivial.

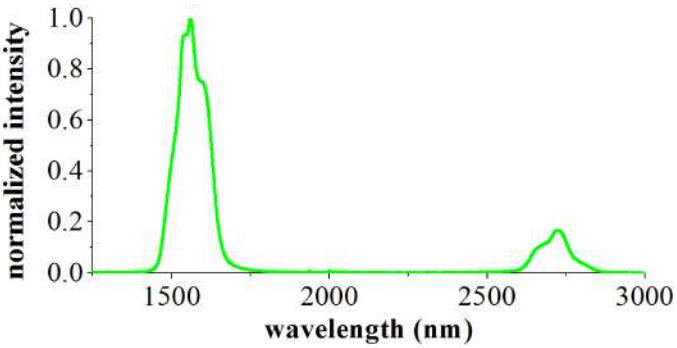


Fig. 3. Normalized fluorescence spectra.

## 6. Conclusion

We demonstrate that the addition of $La_2O_3$ to tellurite glass is a powerful approach to achieve index matching between active and passive glasses. Replacement of ~10% of the passive $La^{3+}$ ions by active $Er^{3+}$ ions resulted in the same index in the near infrared region for both glasses. This will facilitate the development of practical core-doped tellurite MOFs. More generally, this advance will enable the placement of the doped glass anywhere in a MOF with no impact on the fiber's guidance, something that is not possible in more conventional active fibre designs, a feature that could potentially lead to new and more flexible control of fibre laser properties. We have demonstrated that the $Er^{3+}$ absorption intensities and fluorescence lifetimes are not detrimentally affected by the $La_2O_3$ addition, whereas the thermal and crystallization stability are observed to improve in the La-tellurite glass. The loss of the bare fibers demonstrates that the addition of $La_2O_3$ does not impact the material loss. The Er-doped La-glass exhibits strong fluorescence at both 1.5 μm and, to the best of our knowledge, for the first time in tellurite glass at 2.7 μm.

## Acknowledgements

We acknowledge the ARC for their funding (DP20101384); DSTO (Australia) for support and funding to the Centre of Expertise in Photonics and this work; P. Veitch and D. Ottaway at the University of Adelaide, K. Mudge, B. Claire, K. Grant, A. Hemming and D. Lancaster at DSTO for useful discussions; S. Manning, R. Moore at Adelaide University for DSC measurements and fiber drawing, and S. Madden for use of the ANU prism coupler for refractive index measurements. T. Monro acknowledges the support of an ARC Federation Fellowship.